POTENTIAL FOR PHOTOVOLTAIC CELL MATERIAL BY GREEN SYNTHESIS OF SILICON CARBIDE FROM CORN COB THROUGH MAGNESIOTHERMIC REDUCTION

ARWIL NATHANIEL R. ALFONSO, JOEL R. SALAZAR, JUVY J. MONSERATE &
MARILOU M. SARONG
Central Luzon State University, Philippines

ABSTRACT

Corn cobs can be processed chemically to generate new products for electricity employing a simple, low-cost, and environment friendly method. In this article, silicon carbide (SiC) and activated carbon can be synthesized from corn cobs via sol–gel and a chemical activation method, respectively. SiC was synthesized by reacting the synthesized silica and activated carbon with magnesium powder, which served as catalyst at 600 ºC. The SiC was doped with varying amount of Al_2O_3 (0.01, 0.015, 0.02 and 0.1 g), a p-type dopant, via solvothermal synthesis. The undoped SiC was characterized using Scanning Electron Microscopy with Energy Dispersive X-ray Spectroscopy (SEM-EDX) and Fourier Transform Infrared (FTIR). Then, the band-gap energy and conductivity of undoped SiC and p-doped SiC were determined. SEM-EDX and FTIR analysis confirmed the presence of Si–C bond in the synthesized SiC from corn cob. It was observed that p-doped SiC absorbs higher energy in the visible region than undoped SiC. FTIR analysis confirmed the incorporation of the aluminum in the SiC. UV–vis spectroscopy confirmed that the synthesized p-doped SiC exhibits higher absorbance compared with undoped SiC. Aluminum doping also increased absorption bands on the visible region making it more efficient for potential application in photovoltaic (solar) cells because of the decreased band-gap energy and increase in conductivity of p-doped SiC. The ratio of 1:1–2 (SiC:Al) showed the lowest band-gap and highest conductivity with a value of 1.57–1.58 eV and 0.080–0.082 mS/cm compared with the amount of other p-dopants. Statistically, it was found that the 1:1–2 ratio of SiC:Al can be an effective p-junction for the application in photovoltaic (solar) cells.

Keywords: corn cob, p-doped SiC, photovoltaic solar cell, silicon carbide (SiC).

1 INTRODUCTION

Corn is second to rice as the most important crop in the Philippines, with one-third of Filipino farmers depending on corn as their source of livelihood. Corn production in the Philippines as of May 2018 is 2.48 metric tons, which is by 4.66% higher than the production in 2017 [1]. Corn cob (long, hard, and center part of the corn) is an agricultural waste commonly burnt and/or discarded, which leads to greenhouse gas releases, such as carbon dioxide [2]. Burning of agricultural waste is not only considered an economic loss but it also has harmful effects on the environment. Due to its huge availability as a raw material, utilizing corn cob waste as resource could become more economical in preparing activated carbon and silica; this will decrease the waste disposal and also convert corn cob into value-added products [3].

As a renewable raw material, corn cobs from grain maize have potential for the production of activated carbon [4] and silicon dioxide [3] – which are the raw materials for the synthesis of silicon carbide (SiC) [5] for potential application in photovoltaic solar cells.

SiC is a hard and strong semiconductor, which is the only chemical compound of carbon and silicon. It is composed of tetrahedrals of carbon and silicon atoms with strong bonds in the crystal lattice. This produces a very hard and strong material [6]. The most common process to obtain SiC needs high temperatures ranging from 1150 to 1500 ^{0}C, thus requiring high

ISSN: 2056-3272 (paper format), ISSN: 2056-3280 (online), http://www.witpress.com/journals
DOI: 10.2495/EQ-V5-N1-14-23

energy [7]. Solvothermal synthesis is a method that utilizes low temperature (600 ^{0}C) to synthesize p-doped and n-doped semiconductor (i.e. SiC) for p–n junction in photovoltaic solar cells [8]. This method is simple, low-cost, and environment friendly.

A band-gap is the distance between the valence band of electrons and the conduction band. Essentially, the band-gap represents the minimum energy that is required to excite an electron up to a state in the conduction band where it can participate in conduction. The lower energy level is the valence band, and thus, if a gap exists between this level and band-gap, this allows one to visualize the difference between conductors, semiconductors, and insulators. Semiconductors are solids, which exhibit a weak electrical conductivity, which is proportional to the temperature. These materials have energy band structures that are similar to insulators except the energy gap is small enough so that it can be bridged by the Sun in photovoltaic cells [9].

In this study, nanocrystalline SiC material was synthesized. SiC and p-doped SiC were synthesized and their performance (band-gap and conductivity) assessed for the potential application in photovoltaic solar cells.

2 METHODS AND MATERIALS

The procedure followed in this experimental investigation is summarized in the flowchart of Fig. 1.

2.1 Materials

Corncobs from yellow corn were collected from the local market of Talavera. Analytical grade of sodium hydroxide (NaOH) pellets, sulfuric acid (H_2SO_4), magnesium powder, and deionized water were used in the experiment for the synthesis of SiC. Aluminum oxide (Al_2O_3) was used as a p-type dopant of SiC.

2.2 Synthesis of silica carbide from corn cob

Grounded corn cobs were pyrolyzed at 600 ºC to obtain corn cob ash (CCA). A 10 g of CCA was dissolved in 60 mL of 2.5 M NaOH and refluxed at 80 ºC for 3 h. The pH of the cooled solution was adjusted to 7.0 with 2.5 M H_2SO_4 to form silica hydrogel and incubated for 12 h. The gel was centrifuged at 4,000 rpm for 5 min. The supernatant was discarded and the obtained silica was washed with deionized water and oven-dried at 80 ºC (Fig. 2).

2.3 Synthesis of activated carbon powder from corn cob

Grounded corn cobs were pyrolyzed at 600 ºC for 30 min to obtain carbonized corn cob (CCC). A 20 g of CCC was dissolved in 60 mL of 2.5 M NaOH and refluxed at 120 ºC for 3 h. After cooling, the solution was filtered to obtain the solid carbon and oven-dried at 80 ºC. The dried carbon was pyrolyzed at 900 ºC for 1 h and was cooled overnight.

2.4 Synthesis of SiC

SiC synthesis was based primarily on the solid-state method described by Dasog *et al*. [10]. A mixture of silica, activated carbon, and magnesium powder with a ratio of 1:0.2:0.88 (silica:activated carbon:magnesium) was transferred to a crucible. The mixture was pyrolyzed at

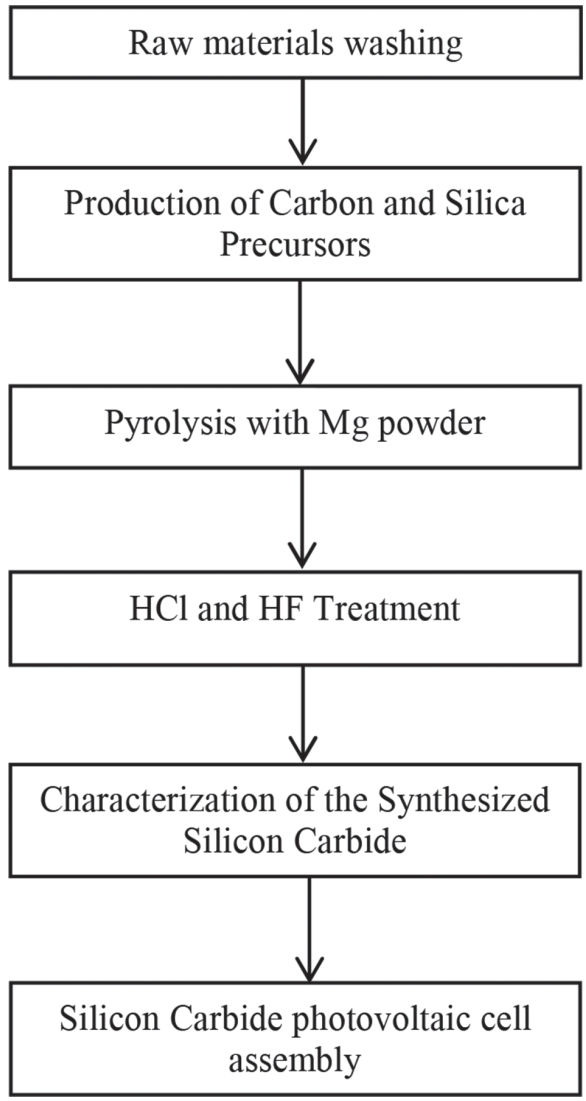

Figure 1: Flowchart from synthesis of silicon carbide (SiC) to production of a SiC photovoltaic cell.

600 ºC for 8 h. The sample was reheated to 500 ºC after cooling at room temperature for 30 min. The resulting solid was acid-leached to 5 M HCl, and the solution was left to stand for 1 h. The solution was filtered, and the solid was washed repeatedly with deionized water and oven-dried overnight at 100 ºC to obtain SiC (Fig. 3).

2.5 Synthesis of p-doped SiC

Approximately 0.01 g (T_1), 0.015 g (T_2), 0.02 g (T_3), and 0.1 g (T_4) of aluminum oxide were mixed in a 4 mL of deionized water and 0.1 g of SiC was added to each container at constant

Figure 2: Macrostructural images of corn cob in different forms (a) dried-bulk corn cobs; (b) ground-corn cobs; (c) carbonized corn cob, and (d) corn cob ash powder pyrolyzed at 600 oC.

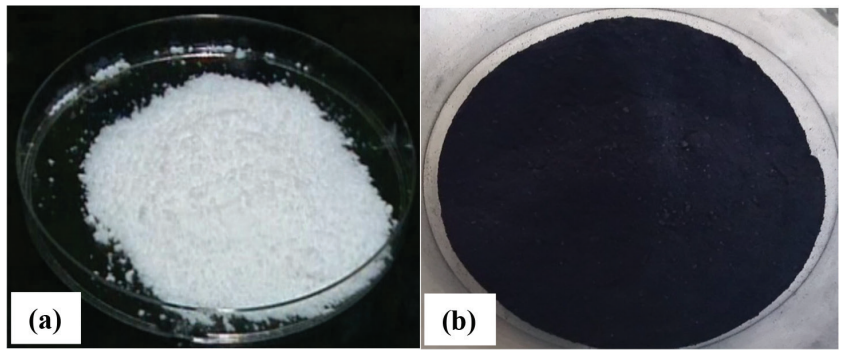

Figure 3: Macrostructural images of (a) silica from corn cob ash; and (b) activated carbon from carbonized corn cob.

stirring for 10 min. The doping process was done via heating the solutions at 180 ºC for 12 h and the resulting Al-doped SiC was cooled overnight (Fig. 4).

2.6 Characterization and performance assessment

Voltammetric measurements were conducted to determine its potential in photovoltaic solar cell application. Cyclic voltammetry was performed to measure the band-gap, efficient charge transfer from donor to acceptor component, and effective charge transport and charge collection at the electrodes.

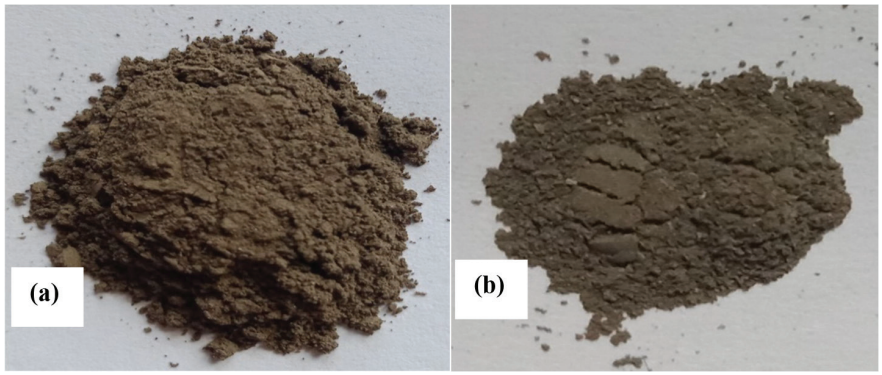

Figure 4. Macrostructural images of synthesized (a) undoped SiC; and (b) P-doped SiC.

3 RESULTS AND DISCUSSION

3.1 Characterization of the synthesized SiC

3.1.1 Scanning Electron Microscopy with Energy Dispersive X-ray Spectroscopy (SEM-EDX) analysis

The SEM graph of the synthesized SiC, shown in Fig. 5, allows the determination of the surface morphology. The SEM showed large particles but irregular in shape. Figure 5 also shows the EDX spectrum of the synthesized SiC and confirmed the presence of Si (highest intensity), C, O, and Mg peaks measured between 0 and 2 keV, which revealed that the SiC was synthesized. Table 1 displays the mass percent of silica and carbon with a value of 60.97% (by weight) and 31.07% (by weight), respectively, indicating the predominant presence of silicon and carbon species in the sample. The presence of residues like oxygen (7.11 wt%), indicated the presence of silica, and trace residual of Mg (0.85 wt%) was also detected because the synthesized SiC was only washed once with HCl resulted in incomplete removal of residues (SiO_2 and Mg).

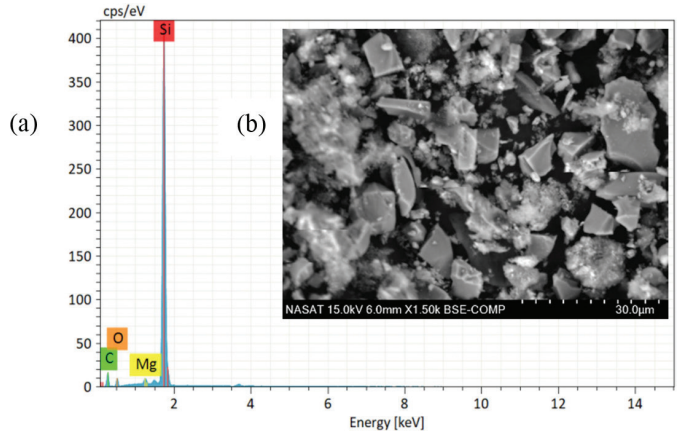

Figure 5. (a) EDX spectra of synthesized silicon carbide; (b) microstructural image of synthesized SiC.

Table 1: Electron dispersive X-ray spectroscopy readings of synthesized SiC.

Element	Atomic Number	Mass Norm. (%)	Atom (%)
Si	14	60.97	41.45
C	6	31.07	49.40
O	8	7.11	8.49
Mg	12	0.85	0.67

3.1.2 Fourier Transform Infrared (FTIR) spectroscopy analyses

The infrared spectrum of the synthesized undoped and doped SiC powder is presented in Fig. 6; this allows the study of the vibration bands of Si–C bond, as well the changes brought about by the substitution of Al_2O_3 in the silicon by SiC. Figure 6 reveals a broad band in the region of 3,000–3,700 cm^{-1} corresponding to the presence of hydroxyl groups that caused stretching vibration of the O–H bond from the silanol groups. (Si–OH) due to adsorbed water molecules on the silica surface (since silica has hygroscopic properties) [3], [12]. Furthermore, the spectrum of Fig. 6 shows a band of Si–O asymmetric stretching vibration appearing at about 1,000–1,100 cm^{-1} [3]. The unique peak in the 1,300–1,500 cm^{-1} region was the C–H bending that might be due to carbon–hydrogen interaction between SiC and H_2O that was adsorbed by the SiC powder. The peaks observed around 800–1,000 cm^{-1} were due to the stretching mode of Si–C [5], which indicated that SiC was synthesized in the experiment.

In Fig. 7, a change in peak was observed, the spectrum displays a diminished peak in the region from 800 to 1,000 cm^{-1} (the SiC), and an enhanced absorption peak in the 1,000–1,200 cm^{-1} region. The strong absorption in the 1,000–1,200 cm^{-1} region corresponds to the stretching mode of Al–O [13], which implies that the aluminum ions were integrated in the synthesized SiC.

3.2 Performance assessment of synthesized undoped SiC and p-doped SiC (Al:SiC)

3.2.1 Band-gap of synthesized and p-doped SiC

Band-gap is the distance between the conduction band and valence band, which determines the conducting ability of a semiconductor. The synthesized SiC powders together with the p-doped SiC powders absorbed radiation in the visible region.

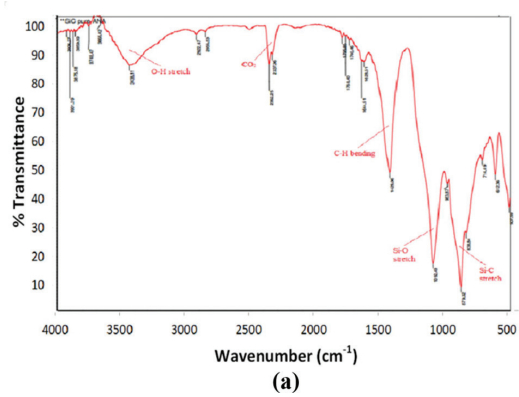

(a)

Figure 6. (a) FTIR Spectrum of synthesized SiC and (b) its functional groups.

Doping the semiconductor with a metal oxide such as Al_2O_3 was intended to create local energy levels within the band-gap of the semiconductor with increase in the absorption bands in the visible region, which makes the semiconductor more efficient in absorbing energy [14]. The band-gaps of the undoped SiC and Al-doped SiC were determined using HITACHI UH5300 UV–Visible Spectrophotometer by measuring the absorption peaks of the synthesized sample in a probable relation to the electronic transition taking place in the conduction band from valence band [14]. Table 2 shows the calculated band-gap energy of synthesized SiC and Al-doped SiC (or p-doped SiC).

Optical absorption analysis demonstrated that p-doped SiC exhibits higher absorption in the visible region compared with undoped SiC. This was due to the p-dopant (Al_2O_3) that altered the lattice structure of the semiconductor (SiC) caused by the replacement of foreign atoms that narrows the band-gap of the synthesized SiC.

Analysis of variance using STAR (Statistical Tool for Agricultural Research Ver. 7.00) showed a significant difference between undoped SiC and doped SiC. The 0.01–0.02 g Al-doped SiC (T_1–T_3) exhibits the lowest band-gap and was found to be significantly different from undoped SiC and 0.1 g Al-doped SiC (T_4). It is noted in Table 2 that the band-gap energy started to decrease from 2.07 to 1.57 eV when 0.01 g of Al_2O_3 was doped in SiC but a significant increase in band-gap energy (1.61 eV) was observed when 0.1 g Al_2O_3 was doped in SiC. An increase in band-gap energy after adding 0.1 g Al_2O_3 may be due to the excess Al but it does not produce enough holes necessary for the lowering of band-gap because of the Mg impurity in the SiC produced. These synthesized Al-doped SiC (T_1–T_4) are considered as an effective p-junction for the possible application in photovoltaic (solar) cells because they satisfied the requirement that their range lies between 1.0 and 1.7 eV for a semiconductor in photovoltaic (solar) cell application.

3.2.2 Conductivity of undoped SiC and p-doped SiC (Al:SiC)

Conductivity defines a material's ability to conduct electricity. Electric current can flow easily through a material with high conductivity. A semiconductor, such as SiC and doped SiC, has intermediate conductivity since it has a narrow band-gap (Table 3), and the band-gap is inversely proportional to conductivity. Table 3 shows the conductivity of undoped and doped SiC that confirms this relationship.

The conductivity of undoped and p-doped SiC was measured using HORIBA SZ-100. Analysis of variance using STAR showed a significant difference between undoped and doped SiC. The 0.01–0.015 g Al-doped SiC (T_1–T_2) was found to be significantly different from undoped SiC (T_0) and 0.02–0.1 g Al-doped SiC (T_3–T_4). The increase of conductivity

Table 2: Band-gap energies of synthesized SiC and p-doped SiC*.

Sample	Band-gap mean (eV)
SiC (T_0)	2.07^a±0.02
0.01 g Al-doped SiC (T_1)	1.57^b±0.03
0.015 g Al-doped SiC (T_2)	1.58^b±0.03
0.02 g Al-doped SiC (T_3)	1.58^b±0.02
0.1 g Al-doped SiC (T_{4d})	1.61^c±0.02

*Mean values with the same letter are not significantly different using STAR at 5%.

Table 3: Conductivity of synthesized undoped SiC and p-doped SiC particles*.

Sample	Conductivity mean (mS/cm)
SiC (T_0)	0.061^{c}±0.003
0.01 g Al-doped SiC (T_1)	0.082^{a} ±0.003
0.015 g Al-doped SiC (T_2)	0.080^{a}±0.002
0.02 g Al-doped SiC (T_3)	0.071^{b}±0.003
0.1 g Al-doped SiC (T_4)	0.069^{b}±0.002

* Means with the same letter are not significantly different using STAR at 5%.

in the p-doped SiC was observed because of the sudden decrease of band-gap. This could be due to the p-dopant using Al_2O_3 that is added to semiconductor (SiC), which produced holes in the valence band. When voltage is applied, the electrons are produced from the valence band and it will jump to the conduction band to produce more electricity. Thus conductivity is enhanced due to doping. Table 3 displays the conductivity trend of the undoped SiC and p-doped SiC. It was observed that the 0.01–0.015 g Al-doped SiC (0.071–0.082 mS/cm) exhibits the highest conductivity among the synthesized SiC since they are not significantly different [15], [16]. However, band-gap energy and conductivity in 0.02 g Al-doped SiC (refer to Table 3) are significantly different to each other because of the greater interfering effect of Mg in the excess 0.05 g of Al_2O_3 in 0.02 g Al-doped SiC that decreased its conductivity even though it has a same band-gap energy value with 0.015 g Al-doped SiC.

Furthermore, when the amount of Al dopant was further increased into 0.02–0.1 g Al, the conductivity of the Al-doped SiC started to decrease. The decrease in the conductivity may be due to the presence of Mg residue in the SiC powder that interfered in the formation of holes brought by the addition of excess aluminum to the SiC material. The effect of Mg impurity may trap the electrons in the valence band and may inhibit the movement of electrons into the conduction band. Thus, the presence of Mg on the surface of SiC tends to agglomerate the SiC particle causing to decrease the conductivity of 0.02 and 0.1 g Al-doped SiC [17].

4 CONCLUSIONS AND RECOMMENDATIONS

SiC and Al-doped SiC were successfully synthesized in this study using solid-state synthesis as supported by SEM-EDX and FTIR spectra. Nanocrystalline SiC was successfully synthesized via the solvothermal method. Compared to that produced by other methods, it is 50% less expensive than conventional silicon cells available in the market.

Performance assessment of undoped and Al-doped SiC was carried out and showed that the 0.01–0.02 g Al-doped SiC has the lowest band-gap (1.57–1.58 eV) and exhibits the highest conductivity (0.080–0.082 mS/cm). Therefore, a mass ratio of 1–2:10 (Al:SiC) was the most efficient p-doped SiC for potential p-junction of photovoltaic (solar) cell.

Based on the findings of the study, the following recommendations are hereby advised:

1. Use of hydrofluoric acid in acid-leaching process for the complete removal of impurities such as silica and magnesium in the SiC for the prevention of decrease in conductivity;
2. Further characterization of p-doped SiC including: SEM to examine the surface morphology, EDS to determine the elemental composition, and X-ray diffraction (XRD) to reveal the crystallinity of the p-doped SiC;

3. Fabrication of synthesized p-doped SiC in a photovoltaic (solar) cell in order to test the actual efficiency of the p-doped SiC in solar absorption;
4. Test the degradation of corn cob (i.e. thermogravimetric analysis); and
5. Conduct a feasibility study on the utilization of corn cob for SiC synthesis.

ACKNOWLEDGMENTS

This study was supported by Physical, Inorganic, and Material Science Laboratory (PIMS-lab), Department of Chemistry, Central State University, Science City of Muñoz, Nueva Ecija.

REFERENCES

[1] Teves, C., *Philippine News Agency*, August 1, 2019, from PH corn production up 4.66% in 1st quarter: https://www.pna.gov.ph/articles/1035104, 2018.

[2] Chanadee, T. & Chaivarat, S., Preparation and characterization of low cost silica powder from sweet corncobs. *Journal of Material and Environmental Science*, **7(7)**, pp. 2369–2374, 2016.

[3] Shim, J., Velmurugan, P. & Oh, B., Extraction and physical characterization of amorphous silica made from corncob ash at variable pH conditions via sol gel processing. *Journal of Industrial and Engineering Chemistry*, **30**, pp. 249–253, 2015. https://doi.org/10.1016/j.jiec.2015.05.029

[4] Abdel Rahim, M.A., Ismail, M. & Abdel Mageed, A.M., Production of carbon and precipitated white nanosilica from rice husk ash. *International Journal of Advanced Research*, **3**(**2**), pp. 491–498, 2015.

[5] Dasog, M., Smith, L., Purkait, T. & Veinot, J., Low temperature synthesis of silicon carbide nanomaterials using solid-state method. *Chemical Communications*, **49**, pp. 7004–7006, 2013.

[6] Negi, Y.S. & Kumar, S., Nanoparticles synthesis from corn cob (xylan) and their potential application as colon-speficic drug carrier. *Macromolecular Symposia*, **320**(**1**), pp. 75–80, 2012.

[7] Ceballos-Mendivil, I.G., Lopez, R.E., Cordova, J.C., Yescas, R.M., Zavala-Rivera, P. & Gonzalez, J.H., Synthesis and characterization of silicon carbide in the application of high temperature solar surface receptors. *Energy Procedia*, **57**, pp. 533–540, 2013. https://doi.org/10.1016/j.egypro.2014.10.207

[8] Mohanraj, K., Kanan, S., Barathan, S. & Sivakumar, G., Preparation and characterization of nano SiO_2 corncob ash by precipitation method. *Optoelectronics and Advanced Materials-Rapid Communication*, **6**(**3**), pp. 394–397, 2012.

[9] Gonzales, A., Hernandez, A., Chaves, C., Castano, V. & Santos, C., Novel crystalline SiO_2 nanoparticles via annelids bioprocessing of agro-industrial wastes. *Nanoscales Research Technology*, **5**(**9**), pp. 9654–9656, 2010. https://doi.org/10.1007/s11671-010-9654-6

[10] Abderrazak, H. & Hmida, E.S.B., Silicon Carbide: Synthesis and Properties. *Properties and Applications of Silicon Carbide*, Chapter 16, 2011. Doi:10.5772/15736

[11] Sharma, S., Jain, K. K. & Sharma, A., Solar cells: in research and applications – a review. *Material Sciences and Applications*, **6**, pp. 1145–1155, 2016. https://doi.org/10.4236/msa.2015.612113

[12] Zhang, Y., Yang, M., Zhan, G. & Dionysiou, D., HNO_3-involved one-step low temperature solvothermal synthesis of N-doped TiO_2 nanocrystals for efficient photo-

catalytic reduction of Cr(VI) in water. *Applied Catalysis B: Environmental*, **142–143**, pp. 249–258, 2013. https://doi.org/10.1016/j.apcatb.2013.05.023

[13] Vahur, S., Teearu, A., Peets, P., Joosu, L. & Leito, I., ATR-FT-IR spectral collection of conservation materials in the extended region of 4000-80 cm–1. *Analytical and Bioanalytical Chemistry*, **408**(**13**), pp. 3373–3379, 2016. https://doi.org/10.1007/s00216-016-9411-5

[14] Nie, S. & Smith, A., Semiconductor nanocrystals: Structure, properties, and band-gap engineering. *Accounts of Chemical Research*, **43**(**2**), pp. 190–200, 2019. https://doi.org/10.1021/ar9001069

[15] Okoronkwo, E.A., Imoisili, P.E. & Olusunle, S.O.O., Extraction and characterization of Amorphous Silica from Corncob Ash by Sol-Gel Method. *Chemistry and Material Research*, **3**(**4**), pp. 68–72, 2013.

[16] Gopal, V.R.V. & Kamila, S., Effect of temperature on the morphology of ZnOnanoparticles: a comparative study. *Applied Nanoscience*, **7**, pp. 75–82, 2017. https://doi.org/10.1007/s13204-017-0553-3

[17] Hirayama, N., Iida, T., Sakomoto, M., Nishio, K. & Hamada, N., Substitutional and interstitial impuriry p-type doping of thermoelectric Mg2Si: a theoretical study. *Science and Technology of Advanced Materials*, **19**, pp. 160–172, 2019. https://doi.org/10.1080/14686996.2019.1580537